New Force Field for Na Cations in Faujasite-Type Zeolites

Eugenio Jaramillo[†] and Scott M. Auerbach*[,†,‡]

Departments of Chemistry and Chemical Engineering, University of Massachusetts, Amherst, Amherst, Massachusetts 01003

Received: April 28, 1999; In Final Form: July 26, 1999

We have developed and validated a new force field for cations in zeolites, which explicitly distinguishes Si and Al atoms, as well as different types of oxygens in the framework. Our new force field gives excellent agreement with experimental data on cation positions, site occupancies and vibrational frequencies. Energy minimizations show that Na cations in site I are not at the centers of hexagonal prisms, but rather are in one of two symmetric S_I sites displaced by about 0.6 Å along the [111] direction. Molecular dynamics (MD) simulations show that most cations are immobile in Na−X and Na−Y on the MD time scale, even at 1000 K. Only Na−X cations in site III′ exhibit diffusive motion at 1000 K, with a self-diffusivity from MD of 3.6 $\times$ 10^{-10} m^2 s^{-1}. The MD simulations also show that cation movement is highly correlated, composed of jumps involving at least 4 cations or more.

1. Introduction

Cation-containing zeolites have recently been found to be effective for separating various hydrofluorocarbon (HFC) mixtures,[1] such as HFC-134 (HF_2C-CF_2H), and HFC-134a (F_3C-CFH_2). To develop an understanding of the factors that control this and other separations, Grey et al.[2] reported a combined NMR and X-ray diffraction study of HFC-134 in Na−Y. Their study suggests that the interaction of HFC-134 with the Na cations is so strong that the HFC induces significant migration of Na(I′) cations into the Na−Y supercage to maximize favorable interactions with the HFC. This result is surprising because cation transport in dry zeolites is typically quite sluggish, only becoming appreciable once the zeolite absorbs water as in ion-exchange applications. This study clearly indicates that dry zeolites cannot be considered as static materials during gas adsorption and transport. To better understand the cation redistribution observed by Grey et al.,[2] we have developed a new force field for cations in zeolites that can be used in dynamics simulations with various silicon to aluminum (Si:Al) ratios.

Na−X and Na−Y are industrially important zeolites with the FAU framework structure, which are distinguished by their Si:Al ratio [Si:Al(X) < 1.5, Si:Al(Y) > 1.5] and consequently by their Na cation content. The extra-framework cations are located in various crystallographic positions, as shown in Figure 1. Site I cations are located in the hexagonal prisms, which connect sodalite cages (β-cages). Site II cations are in the supercage, coordinating with three oxygens from the 6-ring window of the sodalite cage. Site I′ and II′ cations are inside the sodalite cage facing positions I and II, respectively. A unit cell of faujasite contains 16 sites I, and 32 of each I′, II, and II′. Two additional sites have been found in the Na−X supercage: sites III and III′. Cations in site III are located above the 4-ring window while those in site III′ are at the edges of the 4-ring window, i.e., in the 12-ring window. Using single-crystal X-ray diffraction,

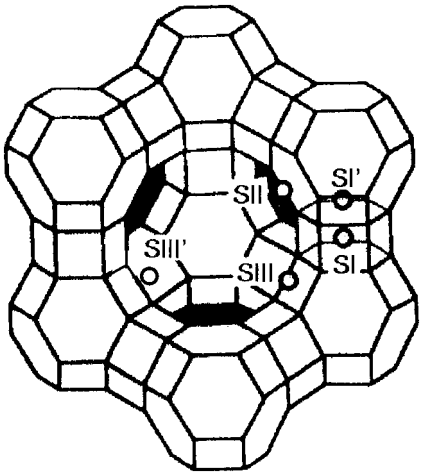

Figure 1. Position of extraframework cations in faujasites.

Olson[3] has observed three distinct positions for cations in site III′ and two for site I′. The Na(III′) site that Olson[3] labels Na6′ corresponds closely to the Na(III′) location found by powder neutron diffraction and molecular mechanics calculations reported by Vitale et al.[4]

A variety of theoretical and computational studies have been reported on the locations of cations in zeolites. Mortier and coworkers have developed lattice models to rationalize the temperature dependence of experimentally determined cation site occupancies.[5,6] Off-lattice Monte Carlo simulations have also been performed to explain and predict cation occupancies[4,7−9] and ordering[10] in zeolites. Electronic structure calculations have been performed to generate potential energy surfaces for cation−frame interactions in sodalite-type zeolites.[11] Molecular dynamics simulations of small amplitude Na and K vibrations in LTA- and FAU-type zeolites have been reported,[12−14] for comparison with vibrational spectra measured for these systems.[14,15] The measured spectra generally contain sharp absorbances between 400−1100 cm^{-1} assigned to zeolite framework vibrational modes, and contain relatively broad bands below 300 cm^{-1} attributed to cation vibrations. The vibrational

* Corresponding author. E-mail: auerbach@chem.umass.edu.
† Department of Chemistry.
‡ Department of Chemical Engineering.

10.1021/jp991387z CCC: $18.00
Published on Web 10/14/1999

spectra simulated with both cation and framework dynamics[14] were in excellent qualitative agreement with experiment. Although fixing the zeolite framework during dynamics simulations slightly sharpened and blue shifted the vibrational spectra, good qualitative agreement with experiment was still obtained. While in principle the simulations can produce cation site-dependent vibrational spectra to facilitate assigning cation vibrational peaks, no clear site-dependent signatures were found.

Using atomistic simulation to model cation transport in dry zeolites is challenging because existing cation−frame force fields are not accurate enough to model correctly all the phase space sampled during cation diffusion. In this article, we develop a single force field for cations in zeolites that can be used with various Si:Al ratios, by explicitly distinguishing Si from Al, and also by distinguishing different types of bridging oxygens. We note that the simulations reported by Vitale et al.[4] and Blake et al.,[11] which also involve force fields that distinguish Si from Al, focus on zeolites with Si:Al = 1, and hence containing only one type of bridging oxygen. Furthermore, the calculations of Vitale et al.[4] fix most of the Na cations in known sites, and hence may not be appropriate for modeling cation mobility. We show below that our model reproduces Na cation occupancies, atomic distances and vibrational frequencies in FAU-type zeolites. We also find that Na(I) cations are displaced from the centers of hexagonal prisms and that cation motion is rather sluggish and highly correlated.

The remainder of this paper is organized as follows: in section II we discuss the methodologies for force field development, cation annealing, classification, and dynamics. In section III we discuss the results from our new force field in comparison with experimental data, and in section IV we give concluding remarks.

2. Methodology

As stated in the Introduction, the goal of this study is to develop a force field for cations in faujasite-type zeolites that is flexible enough to be used for zeolites with various silicon to aluminum (Si:Al) ratios, without the need for reparametrization each time a different Si:Al ratio is used. We will fit the force field to experimentally determined interatomic distances, vibrational spectra, and cation site distributions. The resulting force field will be used to follow cation dynamics in an effort to gain preliminary insights into the transport behavior of cations in dry zeolites.

There are some features in our model that make it different from previous approaches. Several force fields have been reported that use the same charge on silicon and aluminum, i.e., the average "T-site" model.[12−14,16−19] This method may be justified for modeling molecules adsorbed in zeolites when guest atoms remain relatively far from frame atoms. However, we believe that the average T-site method is unrealistic for modeling cations in zeolites, because of the close proximity between cations and frame atoms. In particular, an average T-site model fails to account for the different site III′ positions and occupancies,[3,4,17] and assigns an erroneous symmetric position to cations in site I.[19−21] In addition, vibrational spectra of CO in Na−Y detect three different infrared (IR) frequencies for CO adsorbed near Na(II), corresponding to six-rings containing one, two, or three aluminum atoms.[22] In an effort to model the framework charge distribution more faithfully, we develop a force field that contains different partial charges on silicon and aluminum. We note that Vitale et al. have recently reported a force field for Na−X (Si:Al = 1) using different charges on silicon and aluminum, which accounts for observed cation occupancies at site III′.[4] In this study, most of the 96 Na cations were held fixed at full occupancy in sites I′ and II. While this study provides a useful starting point, our present goal is the development of a force field that reproduces experimental data *without* constraining cations, thereby providing a realistic model for cation dynamics in a variety of zeolites.

TABLE 1: Partial Charges for the Zeolite Potential

species	partial charges
Si	+2.05
Al	+1.75
O_a[a]	−1.20
O_s[b]	−1.025
Na	+1.00

[a] Oxygen bridging an Al atom and a Si atom. [b] Oxygen bridging two Si atoms.

To develop a force field for cationic dynamics, we require atomic charges, short-range potential parameters, algorithms for calculating minimum energy configurations and dynamics, and a method for classifying cationic sites. In what follows, we discuss each of these components.

A. Atomic Charges. Our model explicity distinguishes silicon from aluminum by creating a random distribution of aluminum atoms in the frame that gives the desired Si:Al ratio, obeys Lowenstein's rule[23] precluding adjacent AlO_4 tetrahedra, and involves different partial charges on silicon and aluminum. To develop a single force field that can be used for several Si:Al ratios, different charges were used for oxygen atoms bridging two silicon atoms (O_s), and oxygens bridging one silicon and one aluminum atom (O_a).

For simplicity, we begin our program of force field development reported in this paper by considering only static charges. The most important effect ignored by a cation−frame force field using static charges is the polarization of oxygen by nearby Na cations. In future work, we plan to treat such effects with fluctuating charges,[24−26] which are important for reproducing, e.g., dielectric properties[24] and water−frame interactions.[27]

Atomic charges were assigned by choosing q_{Si}, q_{Al}, and q_{Na} and calculating q_{Os} and q_{Oa}. q_{Os} was obtained using the relation $q_{Si} + 2\ q_{Os} = 0$, while q_{Oa} was determined to make the net system charge equal to zero. We assigned $q_{Na} = +1$, and we find that a difference of 0.3 between q_{Si} and q_{Al} works well, which is consistent with the result found by Herrero[10] for this structure by comparing simulations with ^{29}Si NMR spectra. This value is significantly lower than that assumed by Vitale et al.,[4] i.e., $q_{Si} - q_{Al} = 1.0$, which is likely to overestimate the charge difference between these two atoms. The atomic charges used are shown in Table 1. Many other charge sets were tested, producing either unsatisfactory fitting with experimental results or fitting for just a single Si:Al ratio.

B. Potential. We performed calculations with both flexible and rigid frameworks. The form of the framework potential[28] follows the work of Catlow et al.,[29] involving Coulombic interactions between all the framework atoms, Buckingham interactions between Si/Al atoms and oxygens, and three-body oxygen−Si/Al−oxygen interactions. The potential we used is fully described in ref 28. In what follows, we restrict our discussion to the form of the cation−frame potential. This involves two contributions: a Coulombic interaction between all the atoms and a Buckingham interaction between cations and oxygens, giving $V = V_{Coul} + V_{Buck}$. The Buckingham potential, which models repulsive and dispersive Na−oxygen

TABLE 2: Cation−Framework Short-Range Buckingham Parameters

species[a]	A (eV)	ρ (Å)	C (eV Å^6)
Na−O	5270.0	0.2468	66.0

[a] Same values used both for O_a and O_s.

interactions, is given by

$$V_{\text{Buck}} = \sum_{i>j}[A_{ij}e^{-r_{ij}/\rho_{ij}} - C_{ij}/r_{ij}^6] \quad (1)$$

The interaction between cations and Si/Al atoms is described with a Coulombic term only, because the Coulombic repulsion between Na and Si/Al keeps them well separated, and the polarizabilities of Si and Al are much less than that of oxygen. The values of the potential parameters are summarized in Table 2.

The potential parameters were obtained by fixing the charges according to section IIA and varying the Buckingham parameters by trial and error until calculated cation positions and site occupancies agree semiquantitatively with experimental values. As a further check of the potential, cationic densities of vibrational states were calculated (vide infra) to ensure that they agree qualitatively with experimental vibrational spectra.

C. Cation Annealing. MD-Docker[28] is an annealing procedure that we used in order to obtain the minimum energy configuration for each of the materials studied. Calculations were performed with the program Dizzy[30] for Si:Al ratios varying from 1.0 to 5.3. The modeling was performed in a unit cell containing n Al atoms, $192-n$ Si atoms, $2n$ O_a atoms, $384-2n$ O_s atoms, and n Na atoms, totalling $576+n$ particles. The unit cell is cubic with a lattice parameter of 24.8 Å.[31] Periodic boundary conditions are employed throughout via the periodic image convention. Short-range forces are cut off and shifted at 12 Å, and long-range forces are evaluated with the Ewald summation.[32] An inner cut-off for the Buckingham potential, to avoid its unrealistically attractive form at very short interatomic distances, is unnecessary because this potential remains repulsive up to 25 eV $\approx$ 290000 K.

Each cation annealing consisted of at least 100 independent energy minimizations. Each energy minimization was initiated by a minimum of 1000 steps of 1 fs molecular dynamics (MD) at 1000 K, followed by system cooling using the dynamical minimization algorithm LFOPC developed by Snyman.[33] Simulations were performed with both flexible and rigid zeolite frameworks, giving essentially equivalent results. For this reason, the majority of calculations discussed below were obtained with rigid frameworks to reduce CPU time.

D. Classification Program. In an effort to compare our simulated cation locations to experimentally determined sites and occupancies, we created a program called Clazyx (CLAssification for Zeolites Y and X) that converts three-dimensional coordinates into cationic sites. This program classifies cations based on their positions relative to other atoms, rings, and cages in the FAU structure.

The algorithm initially calculates distances from a given cation to the centers of the 8 supercages, 8 β-cages, and 16 hexagonal prisms using a simplified representation of the FAU structure. Clazyx then finds the supercage, β-cage, and hexagonal prism that are the closest to the cation. At this point, it becomes necessary to use certain length scales that arise naturally from the FAU structure to classify cation sites. If the cation is less than 4.0 Å from the center of the closest hexagonal prism, it is classified as type I or I′, depending on where the cation resides with respect to the six-ring window connecting the hexagonal prism and the closest β-cage, as depicted in Figure 2. To make this distinction, we calculate the distances from the center of the hexagonal prism (hp) to the cation ($d_{\text{hp-cat}}$), and from *hp* to the center of mass of this six-ring window ($d_{\text{hp-ring}}$). If $d_{\text{hp-cat}} < d_{\text{hp-ring}}$, the cation is in a site I; if the opposite is true, the cation is in a site I′.

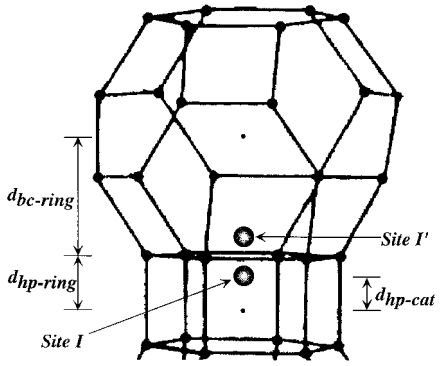

Figure 2. Distances used for classifying cation sites in zeolites.

If the cation is not type I or I′, and its distance to the center of the closest β-cage is less than 5.5 Å, it is classified as II or II′, depending on where the cation resides with respect to the six-ring window connecting the β-cage and the closest supercage. To make this distinction, we calculate the distances from the center of the β-cage (*bc*) to the cation ($d_{\text{bc-cat}}$), and from (bc) to the center of mass of this six-ring window ($d_{\text{bc-ring}}$). If $d_{\text{bc-cat}} < d_{\text{bc-ring}}$, the cation is in a site II′; if the opposite is true, the cation is in a site II.

If the cation is not in sites I, I′, II, or II′, it is either in site III or III′ or it is not in an established site. If it is approximately the same distance (within 0.25 Å) from the four closest T atoms (Si or Al), it is classified as site III. If the cation is not in site III, and is almost the same distance (within 0.10 Å) from the two closest T-atoms (Si or Al), it is classified in site III′ a (corresponding to Olson's[3] type Na5). If it does not meet this criterion, it is classified as being in site III′ b (corresponding to Olson's[3] type Na6′ and Vitale's[4] site III′). In all cases, if the cation is more than 3.0 Å from the closest oxygen, it is not classified. In our minimum energy calculations, all cations have been found in established sites.

E. Dynamics. We performed molecular dynamics (MD) calculations in order to study the extent to which cationic site-to-site jumps are correlated, in an effort to assess the applicability of single-particle kinetic Monte Carlo methods. If indeed these jumps are correlated, then kinetic Monte Carlo cannot be used in a straightforward manner.

As in the case of the energy minimizations, the simulations were performed using the program Dizzy.[30] Molecular dynamics calculations were carried out in the microcanonical ensemble (*NVE*) using a velocity Verlet algorithm with full periodic boundary conditions and a simulation cell containing one unit cell of faujasite (576 atoms) plus the extraframework cations. Simulations were performed at average temperatures near 300 and 1000 K, using a 1 fs time step and Si:Al ratios between 1.0 and 5.3. Total simulation times were at least 500 ps. Cation coordinates and velocities were recorded at least every 50 steps. Cation sites and jumps were monitored every 5, 10, and 50 steps in order to investigate the extent to which site-to-site jumps of many cations are correlated. Histograms showing the extent to which cation motion is correlated were constructed from these data. Mean-square displacements and velocity auto-correlation functions were calculated for each cation after each run. The

TABLE 3: Cation Distribution for $Na_{56}Y$

	simulation	Van Dun[38]	Eulemberger[35]	Jirák[39]	Marra[40]
I	7	7.04	8.00	4.00	9.30
I′	17	13.76	18.88	17.60	13.70
II	25	29.44	30.08	32.00	25.30
other sites	7	3.76	0.04	1.40	3.50
total	56	54.00	57.00	55.00	51.80

TABLE 4: Cation Distribution for $Na_{86}X$ and $Na_{96}X$

	$Na_{86}X$		$Na_{96}X$	
	simulation	Olson[3]	simulation	Vitale[4]
I	1	2.9	3	0
I′	31	29.1	29	32
II	32	31.0	32	32
II′	0	0.0	0	0
III	7	0.0	0	0
III′a	1	10.6	5	0
III′b	14	8.6	27	32
III′c	0	10.6	0	0
total	86	92.9	96	96

densities of vibrational states were computed by Fourier transformation of velocity autocorrelation functions.

3. Results and Discussion

The force field we have developed was used to model faujasites with Si:Al ratios ranging from 1.0 to 5.3. We focus on results for Si:Al = 1.0, 1.2, and 2.4, because these compositions correspond to the most widely available materials. Below we compare our calculated cation site occupancies, interatomic distances and vibrational spectra with experimental data. We also report mean-square displacement calculations for modeling cation diffusion, as well as histograms describing the extent to which cationic motion is correlated.

A. Cation Site Occupancies. The cation site occupancies obtained from energy minimization using our new force field for Na−Y and Na−X are given in Tables 3 and 4, respectively. These occupancies are in very reasonable agreement with experiment, considering the spread in experimental data for these systems. The preferred sites for cations in $Na_{56}Y$ (Si:Al = 2.4) are sites I, I′, and II. Table 3 shows that our model slightly underpredicts the occupancy of site II in $Na_{56}Y$, giving 25 filled sites compared with 28±3 from experiment. Nevertheless, this level of agreement is excellent considering the flexibility and generality of our approach.

Our results for Na−X in Table 4 are in very good agreement with experiment, finding cations predominantly in sites I′, II, and III′. Our results are consistent with Olson's finding of different positions for site III′.[3] We find cations in two variants of site III′, namely, III′a and III′b, corresponding with Olson's Na5 and Na6′, respectively. On the basis of the classification scheme described above, site III′a coordinates most strongly with a single 12-ring oxygen, while site III′b coordinates with two 12-ring oxygens. In agreement with the powder neutron diffraction measurements of Vitale et al.,[4] we find no cations in site III′c (Olson's Na6) and find most III′ cations in site III′ b (Olson's Na6′).

B. Interatomic Distances. Distances from cations to other atoms are shown for $Na_{56}Y$ and $Na_{86}X$ in Table 5. The agreement is excellent with the exception of distances involving Na(I), which is often reported by experiments to reside in the center of the hexagonal prism.[2,31,34,35] Our force field results suggest that Na(I) is not located at the center of the hexagonal prism, but rather is in one of two symmetric S_I sites displaced by about 0.6 Å along the [111] direction. This displacement has been observed recently by Engelhardt[20] using DOR ^{23}Na NMR and confirmed by synchrotron X-ray powder diffraction for Zn cations in zeolite X.[21] This explains why our Na(I)−O(3) and Na(I)−Na(I′) distances are generally shorter than most experimental findings but are in agreement with Engelhardt's results.

C. Vibrational Density of States. The vibrational density of states (VDOS) for cations in different sites in rigid zeolite Na−Y (Si:Al = 2.4) are shown in Figure 3. These results are in broad agreement with infrared measurements on Na−Y,[18] giving absorptions in the 100−300 cm^{-1} range. We have also calculated VDOSs using flexible zeolites (data not shown), finding that significant inhomogeneous broadening smears out features, making site-specific assignments of experimental spectra very difficult.

D. Mean-Square Displacements. Mean-square displacement calculations were performed using MD with our new force field. MSDs for Na−Y at 300 and 1000 K show no appreciable motion of the cations. MSDs for cations in sites I′ and III′ in Na−X at T = 300 and 1000 K are shown in Figure 4a and b, respectively. Figure 4a shows that these cations are essentially immobile at 300 K and that Na(III′) cations have much greater vibrational amplitudes (ca. 1 Å) than those of Na(I′) cations. Figure 4b shows that Na(I′) cations remain immobile even at 1000 K, while Na(III′) cations exhibit diffusive motion, with a diffusion coefficient of approximately 3.6×10^{-10} m^2 s^{-1}. To consider MD as a generally useful tool for probing cationic dynamics and diffusion in Na−X and Na−Y, we require that after a sufficiently long MD run, all cations exhibit the same mobility. This is clearly not the case, as shown in Figure 4a and 4b, forcing us to consider alternative simulation methods for modeling cation dynamics and diffusion.

E. Correlation Histograms. Kinetic Monte Carlo (KMC) is a powerful alternative to molecular dynamics for modeling diffusion when well-defined sites and activated site-to-site jumps can be identified. The basic assumption in most implementations of KMC is that transport is composed of uncorrelated, single particle jumps, which is typically a good approximation for neutral species. However, the long-range forces between Na cations in Na−X and Na−Y may invalidate this assumption, precluding the use of KMC. To test this, we have calculated histograms showing the probability that n cations jump in a particular period of time.

Figure 5a and b show histograms counting the number of cations that move together in Na−X and Na−Y, respectively, during a 50 fs interval at 300 K. Systems dominated by single particle jumps would display histograms with peaks at 0 and 1, showing that in a sufficiently short time either no jumps or single cation jumps have occurred. The histograms in Figure 5a and b exhibit a predominance of group cation jumps in both Na−X and Na−Y. We are unaware of experimental evidence for these correlated cation motions in zeolites, although correlation functions extracted from dynamical neutron scattering experiments[36] could in principle contain signatures of such correlated motions.

Analysis of the underlying MD simulations show rapid movement of Na cations between sites I and I′, across six-ring windows dividing sodalite cages and hexagonal prisms. Similar movements were also found between sites II and II′ and III and III′. At 300 K, no other jumps were detected. At 1000 K, the histograms are essentially the same as those at 300 K, with dynamics consisting primarily of jumps between sites I↔I′, II↔II′ and III↔III′. In addition, rare jumps were observed at

TABLE 5: Cation−Oxygen and Cation-Cation Distances in Faujasites

	simulation	Eulemberger[35]	Fitch[31]	Grey[2]	Lievens[34]	Engelhardt[20]
Na(I)−O(3)	2.11−2.29	2.71	2.71	2.71	2.71	2.3−2.4
Na(I′)−O(3)	2.07−2.27	2.44	2.24	2.32	2.25	
Na(II)−O(2)	2.15−2.36	2.33	2.39	2.34	2.39	
Na(I′)−Na(I)	1.73−1.84	2.61	2.18		2.42	1.58
Na(I′)−Na(II)	4.21−4.63	4.48				

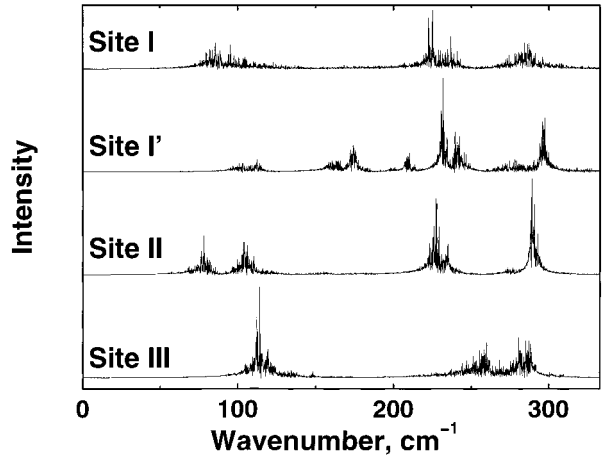

Figure 3. Vibrational densities of states for cations in Na−Y (Si:Al = 2.4) at 300 K.

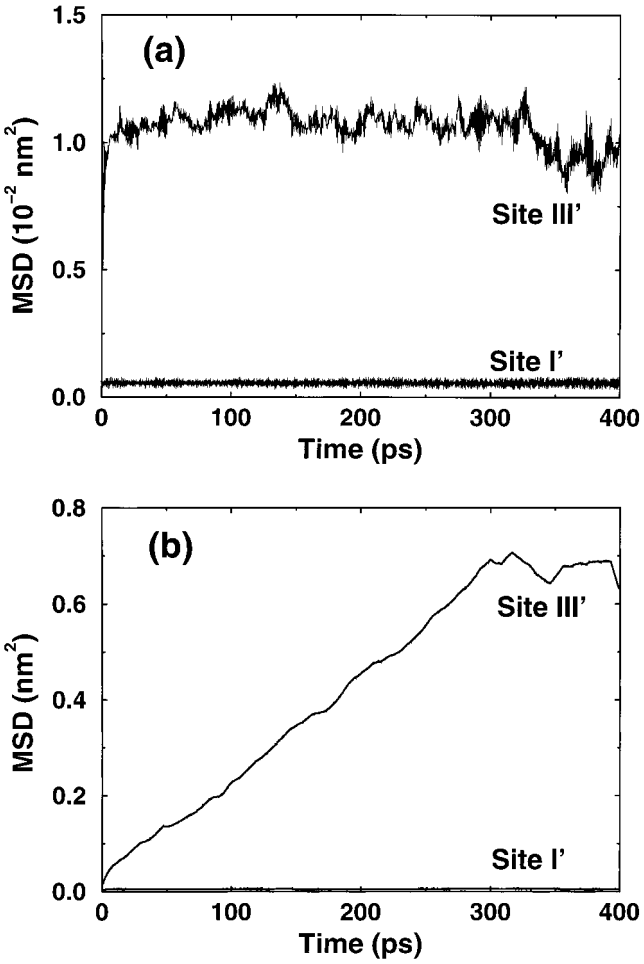

Figure 4. Mean square displacements of selected cations in Na−X (Si:Al = 1.2) at (a) 300 K and (b) 1000 K.

1000 K connecting sites I′ and II to site III′, in qualitative agreement with the measurements of Grey et al.[2] These cation movements are so coordinated that many cations jump simultaneously in an interval as short as 10 fs at 300 K, as shown in Figure 6a and b, for Na−X and Na−Y, respectively. These coordinated movements make it nearly impossible to apply KMC to cation transport, instead requiring methods that can treat sluggish and cooperative dynamics.[37]

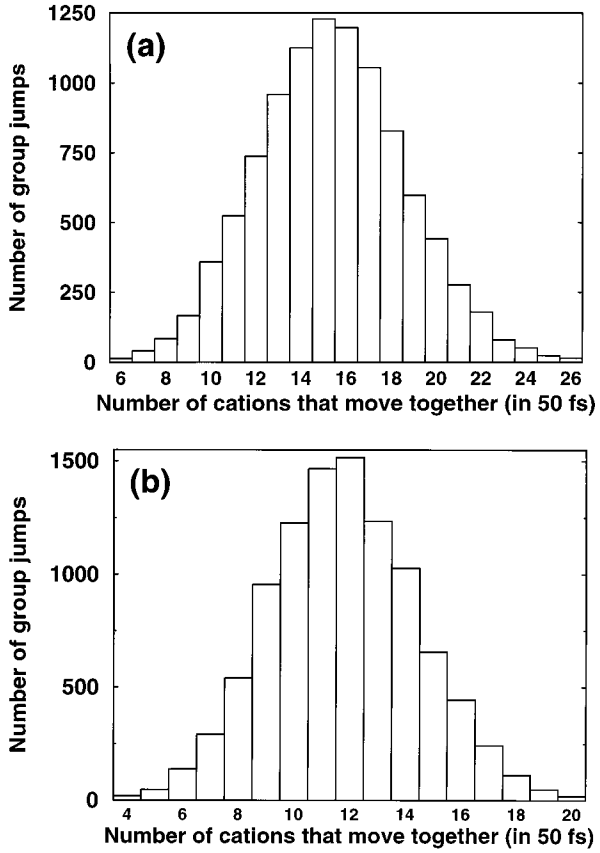

Figure 5. Histogram counting number of jumping cations in (a) Na−X (Si:Al = 1.2) and (b) Na−Y (Si:Al = 2.4), in a 50 fs interval at 300 K.

4. Concluding Remarks

We have developed and validated a new force field for cations in zeolites, which explicitly distinguishes Si and Al atoms, as well as different types of oxygens in the framework. Our new force field gives excellent agreement with experimental data on cation positions, site occupancies, and vibrational frequencies.

Energy minimizations show that Na cations in site I are not at the centers of hexagonal prisms, but rather are in one of two symmetric S_I sites displaced by about 0.6 Å along the [111] direction. Molecular dynamics (MD) simulations show that most cations are immobile in Na−X and Na−Y on the MD time scale, even at 1000 K. Only Na−X cations in site III′ exhibit diffusive motion at 1000 K, with a self-diffusivity from MD of 3.6×10^{-10} m^2 s^{-1}. Rapid exchanges between cations in sites I and I′, II and II′, and III and III′ are observed. The MD simulations also show that cation movement is highly correlated, composed of jumps involving at least 4 cations or more.

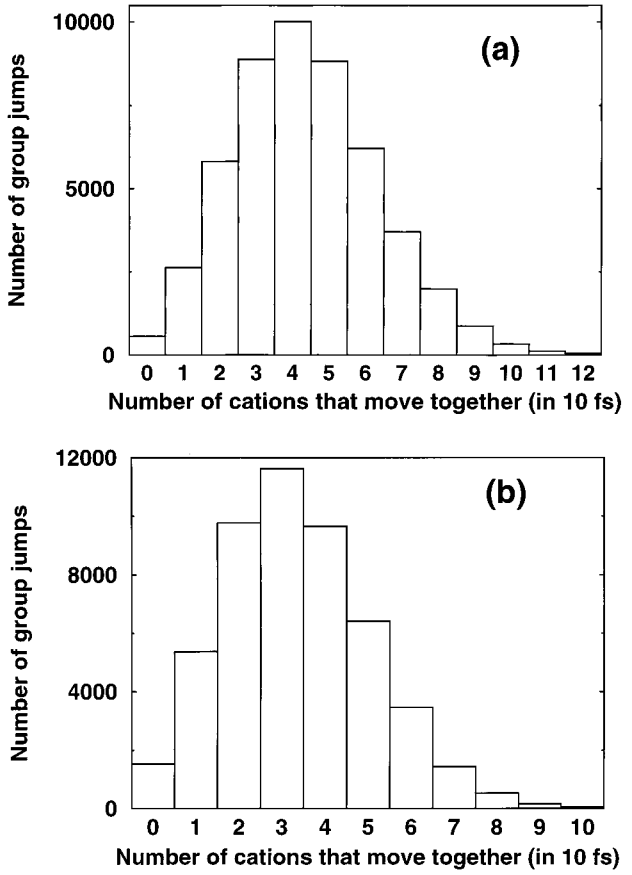

Figure 6. Histogram counting number of jumping cations in (a) Na−X (Si:Al = 1.2) and (b) Na−Y (Si:Al = 2.4), in a 10 fs interval at 300 K.

Many questions remain about cation dynamics in zeolites. In future work we plan to assess the importance of fluctuating charges and flexible frameworks for cation transport. We also plan to study more rigorously the correlated cation movements discussed above, by calculating correlation functions describing the time(s) over which correlations decay. Such calculations will be complicated by the fact that cation motions in dry zeolites present a fundamentally interesting transport system: seemingly intermediate between fluid transport and surface diffusion.

Acknowledgment. The authors thank Prof. C. P. Grey, Prof. A. K. Cheetham, and Prof. W. J. Mortier for very stimulating discussions. S.M.A. thanks the National Science Foundation (Grants CHE-9616019 and CTS-9734153) for generous funding.

References and Notes

(1) Corbin, D. R.; Mahler, B. A. World Patent w.o. 94/02440 (technical report), 1994.
(2) Grey, C. P.; Poshni, F. I.; Gualtieri, A. F.; Norby, P.; Hanson, J. C.; Corbin, D. R. *J. Am. Chem. Soc.* **1997**, *119*, 1981.
(3) Olson, D. H. *Zeolites* **1995**, *15*, 439.
(4) Vitale, G.; Mellot, C. F.; Bull, L. M.; Cheetham, A. K. *J. Phys. Chem. B* **1997**, *101*, 4559.
(5) van Dun, J. J.; Mortier, W. J. *J. Phys. Chem.* **1988**, *92*, 6740.
(6) Smolders, E.; van Dun, J. J.; Mortier, W. J. *J. Phys. Chem.* **1991**, *95*, 9908.
(7) Newsam, J. M.; Freeman, C. M.; Gorman, A. M.; Vessal, B. *Chem. Commun.* **1996**, *16*, 1945.
(8) Gorman, A. M.; Freeman, C. M.; Kolmel, C. M.; Newsam, J. M. *Faraday Discuss.* **1997**, *106*, 489.
(9) Li, B.; Sun, P.; Jin, Q.; Wang, J.; Ding, D. *J. Mol. Structure (THEOCHEM)* **1997**, *391*, 259.
(10) Herrero, C. P.; Ramirez, R. *J. Phys. Chem.* **1992**, *96*, 2246.
(11) Blake, N. P.; Weakliem, P. C.; Metiu, H. I. *J. Phys. Chem. B* **1998**, *102*, 67.
(12) Moon, G. K.; Choi, S. G.; Kim, H. S.; Lee, S. H. *Bull. Korean Chem. Soc.* **1993**, *14*, 356.
(13) Lee, S. H.; Moon, G. K.; Choi, S. G.; Kim, H. S. *J. Phys. Chem.* **1994**, *98*, 1561.
(14) Smirnov, K.; LeMaire, M.; Bremard, C.; Bougeard, D. *Chem. Phys.* **1994**, *179*, 445.
(15) Rodriguez, A. *Vib. Spectrosc.* **1995**, *9*, 225.
(16) Mellot, C. F.; Davidson, A. M.; Eckert, J.; Cheetham, A. K. *J. Phys. Chem. B* **1998**, *102*, 2530.
(17) Auerbach, S. M.; Bull, L. M.; Henson, N. J.; Metiu, H. I.; Cheetham, A. K. *J. Phys. Chem.* **1996**, *100*, 5923.
(18) Krause, K.; Geidel, E.; Kindler, J.; Forster, H.; Smirnov, K. S. *Vibr. Spectrosc.* **1996**, *12*, 45.
(19) Schrimpf, G.; Schlenkrich, M.; Brickmann, J. *J. Phys. Chem.* **1992**, *96*, 7404.
(20) Engelhardt, G. *Microporous Mater.* **1997**, *12*, 369.
(21) Ciraolo, M. F.; Norby, P.; Hanson, J. C.; Corbin, D. R.; Grey, C. P. *J. Phys. Chem. B* **1999**, *103*, 346.
(22) Knözinger, H.; Huber, S. *J. Chem. Soc., Faraday Trans.* **1998**, *94*, 2047.
(23) Newsam, J. M. In *Solid State Chemistry: Compounds*; Cheetham, A. K., Day, P., Eds.; Oxford University Press: Oxford, 1992; pp 234−280.
(24) Jackson, R. A.; Catlow, C. R. A. *Mol. Simul.* **1988**, *1*, 207.
(25) Rick, S. W.; Stuart, S. J.; Berne, B. J. *J. Chem. Phys.* **1994**, *101*, 6141.
(26) Demiralp, E.; Cagin, T.; Goddard, W. A., III *Phys. Rev. Lett.* **1999**, *82*, 1708.
(27) Kitao, O.; Demiralp, E.; Cagin, T.; Dasgupta, S.; Mikami, M.; Tanabe, K.; Goddard, W. A., III *Comput. Mater. Sci.* **1999**, *14*, 135.
(28) Auerbach, S. M.; Henson, N. J.; Cheetham, A. K.; Metiu, H. I. *J. Phys. Chem.* **1995**, *99*, 10600.
(29) Catlow, C. R. A.; Freeman, C. M.; Vessal, B.; Tomlinson, S. M.; Leslie, M. *J. Chem. Soc., Faraday Trans.* **1991**, *87*, 1947.
(30) Henson, N. J. PhD thesis, Oxford University, 1996.
(31) Fitch, A. N.; Jobic, H.; Renouprez, A. *J. Phys. Chem.* **1986**, *90*, 1311.
(32) Allen, M. F.; Tildesley, D. J. *Computer Simulation of Liquids;* Oxford Science Publications: Oxford, 1987.
(33) Snyman, J. A. *Comput. Math. Appl.* **1989**, *17*, 1369.
(34) Lievens, J. L.; Mortier, W. J.; Verduijn, J. P. *J. Phys. Chem.* **1992**, *96*, 5473.
(35) Eulemberger, G. R.; Shoemaker, D. P.; Keil, J. G. *J. Phys. Chem.* **1967**, *71*, 1812.
(36) Jobic, H.; Kärger, J.; Bee, M. *Phys. Rev. Lett.* **1999**, *82*, 4260.
(37) Voter, A. *J. Chem. Phys.* **1997**, *106*, 4665.
(38) van Dun, J. J.; Dhaeze, K.; Mortier, W. J. *J. Phys. Chem.* **1988**, *92*, 6747.
(39) Jirák, Z.; Vratislav, S.; Bosácek, V. *J. Phys. Chem. Solids* **1980**, *41*, 1089.
(40) Marra, G. L.; Fitch, A. N.; Zecchina, A.; Ricchiardi, G.; Salvalaggio, M.; Bordiga, S.; Lamberti, C. *J. Phys. Chem. B* **1997**, *101*, 10653.